Simultaneous traveling convection vortex events and Pc1 wave bursts at cusp latitudes observed in Arctic Canada and Svalbard

J. L. Posch,[1] M. J. Engebretson,[1] A. J. Witte,[1,2] D. L. Murr,[1] M. R. Lessard,[3] M. G. Johnsen,[4] H. J. Singer,[5] and M. D. Hartinger[6]

Received 13 June 2013; revised 30 September 2013; accepted 30 September 2013; published 18 October 2013.

[1] Traveling convection vortices (TCVs), which appear in ground magnetometer records at near-cusp latitudes as solitary ~5 mHz pulses, are a signature of dynamical processes in the ion foreshock upstream of the Earth's bow shock that can stimulate transient compressions of the dayside magnetosphere. These compressions can also increase the growth rate of electromagnetic ion cyclotron (EMIC) waves, which appear in ground records at these same latitudes as bursts of Pc1 pulsations. In this study we have identified TCVs and simultaneous Pc1 burst events in two regions, Eastern Arctic Canada and Svalbard, using a combination of fluxgate magnetometers and search coil magnetometers in each region. By looking for the presence of TCVs and Pc1 bursts in two different sequences, we have found that the distribution of Pc1 bursts was more tightly clustered near local noon than that of TCV events, that neither TCVs nor Pc1 bursts were always associated with the other, and even when they occurred simultaneously their amplitudes showed little correlation. Magnetometer data from GOES-12 were also used to characterize the strength of the magnetic compressions at geosynchronous orbit near the magnetic equator. Compressions >2 nT at GOES-12 occurred during 57% of the Canadian TCV events, but during ~85% of the simultaneous TCV/Pc1 burst events. There was again little evident correlation between TCV and GOES-12 compression amplitudes. We have also documented unusually low EMIC wave activity during this deep solar minimum interval, and we attribute the low occurrence percentage of combined events in this study to this minimum.

Citation: Posch, J. L., M. J. Engebretson, A. J. Witte, D. L. Murr, M. R. Lessard, M. G. Johnsen, H. J. Singer, and M. D. Hartinger (2013), Simultaneous traveling convection vortex events and Pc1 wave bursts at cusp latitudes observed in Arctic Canada and Svalbard, *J. Geophys. Res. Space Physics*, *118*, 6352–6363, doi:10.1002/jgra.50604.

1. Introduction

[2] Interactions between the solar wind and Earth's magnetosphere continue to be the subject of study despite decades of focused effort and numerous satellite missions. As is necessary in a field where passive observation is the rule rather than controlled experimentation, both event studies and large statistical studies have played a role in developing our current understanding of the complex interaction that occurs as the solar wind plasma interacts with Earth's bow shock, passes through it and the magnetosheath, and then interacts with Earth's magnetosphere.

[3] Localized transient reconnection events (flux transfer events) were the first category of small-scale transient events to be identified using ISEE satellite data as frequent occurrences along the dayside magnetopause [*Russell and Elphic*, 1979]. Solitary bipolar perturbations of a few minutes duration were interpreted as instances of the localized reconnection of flux tubes of solar wind and magnetospheric origin. Single-point and conjugate ground-based magnetometer observations near the magnetic foot point of the dayside open-closed field line boundary (the low-altitude cusp) soon revealed similar solitary, bipolar perturbations [e.g., *Lanzerotti et al.*, 1991]. These magnetic impulse events (MIE) were originally viewed as the ground signatures of the flux transfer events observed by ISEE. However, perturbations observed by arrays of ground-based magnetometers at near-cusp latitudes [*McHenry and Clauer*, 1987; *Friis-Christensen et al.*, 1988; *Glassmeier et al.*, 1989] showed that the observed vortical motions of ionospheric equivalent flows were not consistent with theoretical

[1]Department of Physics, Augsburg College, Minneapolis, Minnesota, USA.
[2]Now at Cargill, Inc., Minnetonka, Minnesota, USA.
[3]Space Science Center, University of New Hampshire, Durham, New Hampshire, USA.
[4]Tromsø Geophysical Observatory, University of Tromsø, Tromsø, Norway.
[5]Space Weather Prediction Center, NOAA, Boulder, Colorado, USA.
[6]Department of Atmospheric, Oceanic, and Space Sciences, University of Michigan, Ann Arbor, Michigan, USA.

Corresponding author: J. L. Posch, Department of Physics, Augsburg College, 2211 Riverside Ave, Minneapolis, MN 55454, USA. (posch@augsburg.edu)

2169-9380/13/10.1002/jgra.50604

pictures of the path of flux tubes that had reconnected near the nose of the magnetosphere. These ionospheric vortical patterns and flow directions (tailward along the open-closed boundary) were documented by *Lühr and Blawert* [1994] and *Lühr et al*. [1996], and using data from the Magnetometer Array for Cusp and Cleft Studies (MACCS) array by *Zesta et al*. [1999, 2002] and *Murr et al*. [2002]; they were also modeled by *Kivelson and Southwood* [1991] and *Lysak et al*. [1994] as consequences of fluctuations in the position of the magnetopause, driven by variations in solar wind pressure rather than by reconnection.

[4] These traveling convection vortex (TCV) events have been the subject of numerous studies, and the current consensus is that most, if not all, of these events are not signatures of FTEs or even of large-scale fluctuations in the solar wind but of instabilities generated in the ion foreshock just upstream of Earth's bow shock that cause localized pressure impulses to impinge on the dayside magnetosphere. These impulses in turn generate transient field-aligned currents that close through the very high latitude dayside ionosphere (e.g., the observational studies of *Vorobjev et al*. [1999]; *Moretto et al*. [2002]; *Murr and Hughes* [2003]; *Kataoka et al*. [2003]).

[5] These localized pressure pulses produce other signatures in addition to transient field-aligned currents and vortical motions in the ionosphere. Transient auroral brightenings were identified during several events [*Mende et al*., 1990, 2001; *Sitar et al*., 1998; *Vorobjev et al*., 2001; *Massetti*, 2005; *Fillingim et al*., 2011] as well as nearly simultaneous bursts of narrowband Pc1 waves, with typical frequencies from 0.2 to 1.0 Hz [*Arnoldy et al*., 1988, 1996]. Recent observations from Svalbard reported by *Engebretson et al*. [2013] showed both of these additional signatures and in addition reported both satellite and ground-based observations of precipitating protons in association with the Pc1 waves.

[6] Signatures of transient dayside compressions have also been observed at GOES 5 and GOES 6 at geosynchronous orbit [e.g., *Fairfield et al*., 1990; *Sanny et al*., 2001]. *Fairfield et al*. [1990] used simultaneous data from the AMPTE IRM satellite upstream of the bow shock to show that the eight events they analyzed were associated with solar wind/foreshock/bow shock interactions, and *Sanny et al*. [2001] used IMF and solar wind data simultaneous with 87 transient events observed simultaneously by both GOES spacecraft to infer that a significant fraction of them, at least, were produced by pressure pulses generated in the foreshock/bow shock region.

[7] *Arnoldy et al*. [1988] were the first to note that bursts of Pc1 pulsations often occurred in association with the long-period solitary transients discussed above. *Arnoldy et al*. [1988] identified 280 cases of single-pulse Pc5 waves at Sondrestromfjord, Greenland, with amplitude exceeding 100 nT and found that 60% of them were accompanied by simultaneous Pc1 bursts. In 20% of these cases, similar activity was seen at the nearly magnetically conjugate South Pole station in Antarctica. *Arnoldy et al*. [1988] pointed out that the large scale Pc5 pulses were easily identified, suggesting that reconnection was not likely since the pulses would be difficult to identify during disturbed magnetic conditions. They thus suggested that the signatures on the ground which were coincident with Pc1 bursts might be the result of solar wind pressure increases acting on the magnetosphere rather than flux transfer events.

[8] A follow up study by *Arnoldy et al*. [1996] used search coil magnetometers at Sondrestromfjord (Greenland), Iqaluit (Canada), and South Pole Station (Antarctica). They found that the long-period magnetic impulses propagated in longitude consistent with TCV models. In 70% of these events, a Pc1 burst occurred simultaneously, and, of these events, 50% were identified also in the conjugate hemisphere. This study also found that there was no consistent phase relationship between the time of maximum amplitude of the Pc1 bursts and the time of maximum amplitude of the MIE/TCV.

[9] *Arnoldy et al*. [1996] concluded that as isolated MIE/TCV events move down the flanks of the magnetosphere at a speed roughly equal to that of the magnetosheath flow velocity, they create conditions well within the magnetosphere that can generate ion cyclotron instabilities to produce localized bursts of Pc1 waves. Consistent with this conclusion, *Pilipenko et al*. [1999] presented an example of coordinated motion of a TCV and an associated Pc1 burst at its leading edge across five longitudinally spaced cusp-latitude stations of the MACCS array in Arctic Canada.

[10] In both of the Arnoldy et al. studies, TCV events were identified first and search coil data were subsequently scanned to search for Pc1 bursts. This identification sequence implicitly suggests a causal relationship between the two phenomena, such that only those Pc1 bursts associated with TCVs were identified. To our knowledge, no prior statistical study has explored the various occurrence possibilities for these two phenomena: Do Pc1 bursts accompany some but not all TCVs; do TCVs accompany some but not all Pc1 bursts; are both TCVs and Pc1 bursts generated by some common causal phenomenon (but with an occurrence probability less than unity, dependent on other physical factors); or do TCVs and Pc1 bursts occur independently? In order to begin to address these questions, associations between TCVs and Pc1 wave bursts were analyzed in two different ways using the two data sets obtained in Eastern Canada and at Svalbard: identify TCVs then search for concurrent Pc1 events; identify Pc1 events then search for TCVs.

[11] Section 2 describes the ground-based and satellite-based magnetometer data sets in Arctic Canada and on Svalbard that were used in this study, and section 3 presents four example events. Section 4 presents a statistical analysis of the combined TCV and Pc1 burst data sets from both regions as well as a statistical comparison of compressional events at GOES-12 to TCVs observed by MACCS. Section 5 presents a discussion and summary of our findings and places them in the context of the deep minimum in solar activity during the period of these observations.

2. Data Set and Procedure

[12] The magnetic field data used in this study were recorded in two regions, Eastern Arctic Canada and Svalbard, Norway, both at nominal cusp latitudes (Table 1 and Figure 1). The Magnetometer Array for Cusp and Cleft Studies (MACCS) records DC vector magnetic field data at a two-dimensional array of sites in Arctic Canada, at a cadence of two samples/s [*Hughes et al*., 1995; *Engebretson et al*., 1995]. Two search coil magnetometers operated by the University of New Hampshire and Augsburg College, which record the time derivative (dB/dt) of the vector field 10 times per second, are located near the eastern end of the MACCS array, at Iqaluit,

Table 1. Locations of Fluxgate and Search Coil Magnetometers Used in This Study[a]

Station	Instrument	Geographic Latitude	Geographic Longitude	Geogmag Latitude	Geogmag Longitude	UT of Noon MLT	L Shell
			Eastern Arctic Canada and adjacent and conjugate sites				
Cape Dorset	Fluxgate	64.2°N	283.4°E	73.25°N	2.12°E	16:55	12.2
Iqaluit	Search coil	63.8°N	291.4°E	72.1°N	14.7°E	16:10	10.7
Sondrestromfjord	Search coil	67.0°N	309.3°E	73.4°N	33.4°E	14:55	12.4
South Pole	Search coil	90°S	—	74.3°S	18.6°E	15:36	13.8
AGO-P2	Search coil	85.7°S	313.6°E	70.2°S	19.6°E	15:31	8.8
AGO-P3	Search coil	82.8°S	28.6°E	72.1°S	40.6°E	14:03	10.8
			Svalbard, Norway				
Ny Ålesund	Fluxgate/ Search coil	78.9°N	11.9°E	76.4°N	110.1°E	9:00	Cap
Longyearbyen	Fluxgate/ Search coil	78.2°N	16.0°E	75.4°N	111.1°E	8:56	15.9
Hornsund	Fluxgate/ Search coil	77.0°N	15.6°E	74.3°N	108.7°E	9:05	13.9
			Satellite Foot Point				
GOES-12	Fluxgate	57.2°N	281.2°E	67.2°N	350.7°E	17:00	6.8

[a]Corrected geomagnetic coordinates and universal time (UT) of local magnetic noon (MLT) have been computed for epoch 2008 and an altitude of 100 km using the NSSDC Modelweb facility (http://omniweb.gsfc.nasa.gov/vitmo/cgm_vitmo.html).

Nunavut, Canada, and Sondrestromfjord, Greenland. Search coil magnetometers are also located at several roughly conjugate sites in Antarctica. These include South Pole Station and several automated geophysical observatories that are part of the PENGUIn array [*Engebretson et al.*, 1997].

[13] On Svalbard, the International Monitor for Auroral Geomagnetic Effects (IMAGE) fluxgate magnetometer array [*Lühr*, 1994] extends from nominal cusp latitudes on Svalbard to auroral zone latitudes throughout Fennoscandia and samples the vector magnetic field every 10 s. Four University of New Hampshire/Augsburg College search coil magnetometers are also deployed on Svalbard; these also record dB/dt 10 times per second [*Engebretson et al.*, 2009].

[14] Geomagnetic field conditions at geostationary orbit are determined using vector fluxgate magnetometer data from the GOES-12 spacecraft [*Singer et al.*, 1996], located with foot point near the eastern end of the MACCS array. Table 1 and Figure 1 show the location of these magnetometer sites as well as the magnetic foot point of GOES-12.

[15] In the first part of this study we identified TCVs of $\geq$ 50 nT peak-to-peak (p-p) amplitude by visually inspecting daily line plots of fluxgate magnetometer data from the MACCS site Cape Dorset from 2008 through the first 7 months of 2010. Line plots with time scales of 30 min from Cape Dorset and one additional longitudinally separated station were used to confirm the occurrence and azimuthal motion of the TCV. Pc1 bursts were visually identified using a combination of spectrograms and line plots from Iqaluit, Sondrestromfjord, and South Pole for identified TCV events. To be considered as an event, the Pc1 burst needed to be simultaneous with the TCV envelope, isolated from other Pc1 activity in time

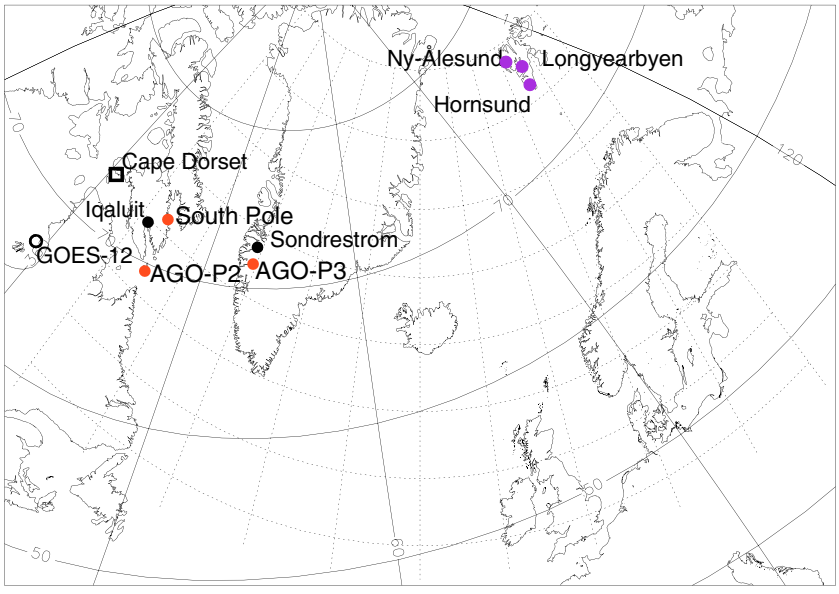

Figure 1. Map showing the arctic locations of the Cape Dorset fluxgate magnetometer (open square), northern hemisphere search coil magnetometers at Iqaluit and Sondrestromfjord (black circles) and Svalbard (purple circles), and the conjugate location of the Antarctic search coil magnetometers (red circles). The mapped footprint of the GOES-12 satellite is shown as an open circle based on data from http://sscweb.gsfc.nasa.gov/.

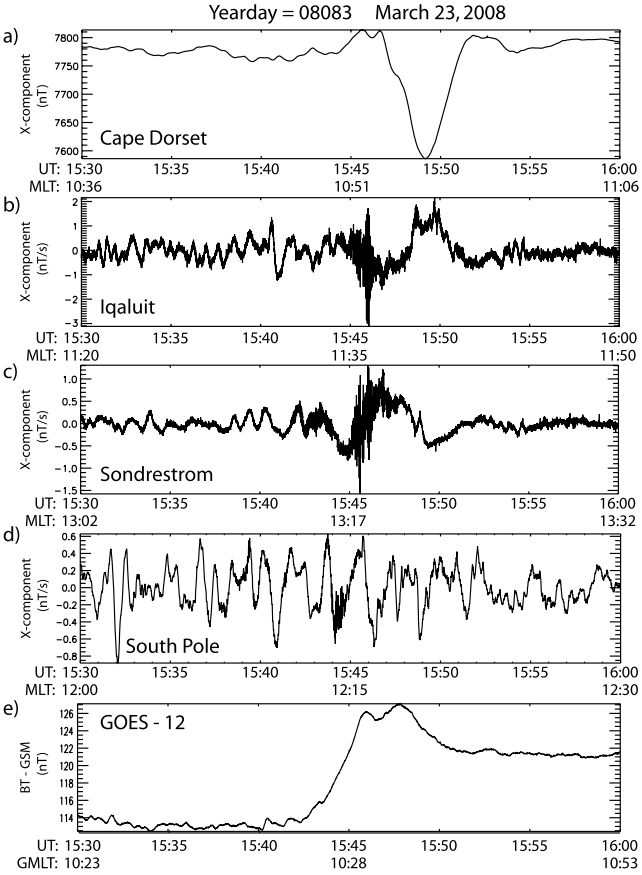

Figure 2. Line plots of magnetic field data from 1530 to 1600 UT 23 March 2008. (a) The X component (north-south) of B at Cape Dorset. The X component (north-south) of dB/dt at (b) Iqaluit (Canada), (c) Sondrestromfjord (Greenland), and (d) South Pole Station, Antarctica, respectively. (e) The magnetic field magnitude at GOES-12 in geosynchronous orbit. The magnetic local time is indicated below the plot for each station.

or power, and identified at one or more of the above search coil locations with amplitude ≥ 0.2 nT/s peak to peak. In the second part of the study, we reversed the order of identification by starting with Pc1 bursts occurring at the Svalbard search coil sites, using the same amplitude thresholds, during the same time period of January 2008 to July 2010. After Pc1 bursts were identified, IMAGE magnetometer data were scanned to search for simultaneous TCVs with peak-to-peak amplitude ≥ 50 nT.

3. Example Events

[16] Sections 3.1–3.3 show examples of TCV events identified at the Eastern Canadian MACCS site of Cape Dorset, along with simultaneous observations of Pc1 wave bursts (or their absence) from Arctic and Antarctic sites at similar magnetic longitudes and latitudes. Also shown are plots of the total magnetic field recorded at GOES-12 during these intervals. Section 3.4 shows an example of a Pc1 burst recorded at Longyearbyen, Svalbard (and observed by each of the three Svalbard search coil magnetometers operating on this day), as well as data from three stations of the IMAGE array during this interval showing a simultaneous TCV.

[17] Although these events were selected to be representative of various features evident in our larger ground-based data set, it was subsequently found that IMF conditions for each event were consistent with the formation of an ion foreshock instability. Detailed analysis of the upstream data for these events, however, is beyond the scope of this study.

3.1. Event 1: 23 March 2008

[18] On 28 March 2008, a ~200 nT p-p TCV was observed in the north-south (X) component of the fluxgate magnetometer data from Cape Dorset (Figure 2a). During this event, a Pc1 wave burst occurred from ~1542 to ~1548 UT in search coil magnetometer data from Iqaluit and Sondrestromfjord, with nearly simultaneous (to within 1 min) peak-to-peak amplitudes of 4.4 and 2.1 nT/s, respectively (Figures 2b and 2c). A TCV signature appeared in the search coil data as well, first at Sondrestromfjord and ~3 min later at Iqaluit, but with much lower amplitude and different waveform than at Cape Dorset (primarily because search coils respond to dB/dt). The peak of the Pc1 burst coincided with the leading downward transition of the TCV at Iqaluit but with the upward transition of the TCV at Sondrestromfjord. Although only very weak ~0.4 nT/s p-p Pc1 wave activity was observed at South Pole Station (Figure 2d), its presence indicates, consistent with earlier observations by *Arnoldy et al.* [1988] and with the third example to be shown here (Figure 4), that such Pc1 bursts appear at near-cusp locations in both hemispheres, but with possible timing offsets of up to ~3 min.

[19] Comparison of the timing of the TCV signatures at SDY and IQA indicated westward and dawnward propagation of this TCV with a speed of 5 km/s. Comparison of the CDA data with fluxgate magnetometer data from Iqaluit (not shown) also indicated westward and dawnward propagation, with a speed of ~3 km/s.

[20] The total magnetic field at GOES-12, in geostationary orbit near local noon, is shown in Figure 2e. An increase in B of 14 nT ending about 1546 UT coincided with the Pc1 burst and the onset of the TCV observed on the ground.

[21] Geomagnetic conditions during this event were quiet: $Kp = 1$ and $Dst = -5$ nT. Time-shifted OMNI solar wind data (not shown) indicated that the IMF cone angle was above 65° from 1530 to 1549 UT (after the onset of the TCV and Pc1 burst), at which time it dropped quickly to ~45° for ~2 min, before increasing slightly to values near 50° until 1556 UT. The solar wind velocity was relatively steady near 480 km/s, with dynamic pressure of 2 nPa, before and during the TCV event. The four Cluster spacecraft, which were located 18 R_E upstream of Earth but ~10 R_E away from the Sun-Earth line, showed similar variations. These upstream observations suggest that the source of the TCV was not a large-scale solar wind pressure increase, but the available spacecraft data appear to be insufficient to determine whether the source was a triggered or spontaneous hot flow anomaly or was simply indeterminate.

3.2. Event 2: 20 June 2008

[22] This TCV event is an example of one during which there was no evidence of a Pc1 burst at any of the search coil locations used in this study. A double-pulsed ~150 nT p-p TCV event occurred from 1810 to 1820 UT as shown in Figure 3a.

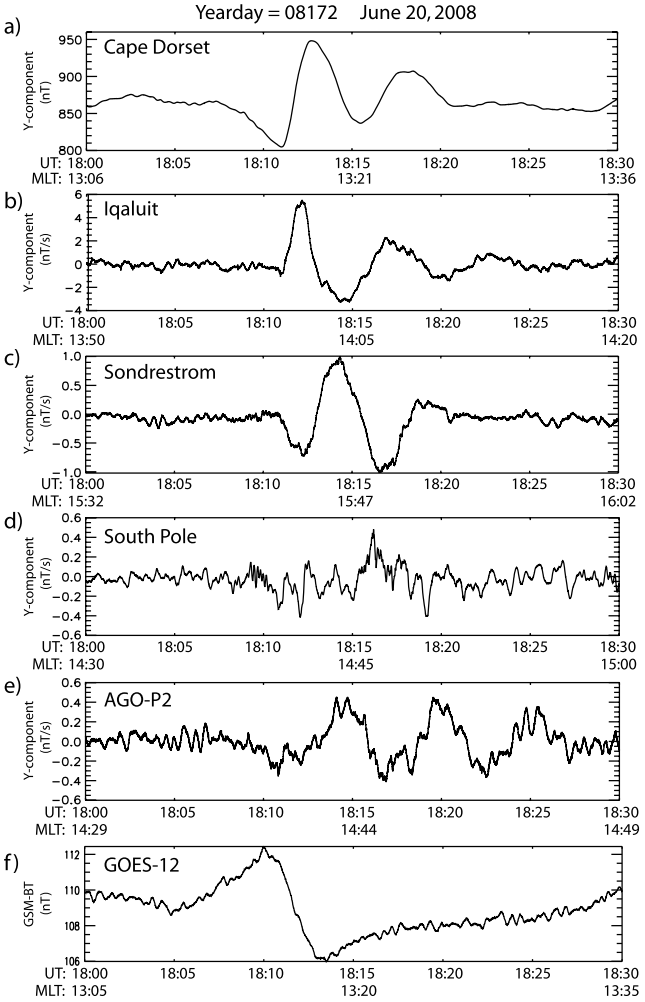

Figure 3. Line plots of magnetic field data from 1800 to 1830 UT 20 June 2008, as in Figure 2. The dB/dt data from two northern hemisphere sites: (b) Iqaluit and (c) Sondrestromfjord; and the dB/dt data from two Antarctic sites: (d) South Pole Station and (e) AGO-P2.

No Pc1 wave bursts with amplitude above the ~0.2 nT/s noise level were observed at Iqaluit, Sondrestromfjord, South Pole, or Automatic Geophysical Observatory (AGO)-P2 (Figures 3b, 3c, 3d, and 3e), but clear TCV signatures appeared in the Iqaluit and Sondrestromfjord data. Comparison of these TCV signatures, as well as comparison of TCV signatures in the Cape Dorset and Iqaluit fluxgate data (not shown), indicated eastward (duskward) TCV propagation with speeds of 7.5 and 6.5 km/s, respectively. Figure 3f shows the magnetic field magnitude observed by GOES-12, showing an increase of ~3 nT in the total field strength near the time of TCV onset, followed by a ~7 nT decrease.

[23] Geomagnetic conditions during this event were again relatively quiet: $Kp = 2-$ and $Dst = -20$ nT. Time-shifted OMNI data (not shown) revealed a very steady solar wind flow speed of 560 km/s, a low solar wind flow pressure of ~1.0 nPa, and a mostly radial IMF (with cone angle $< 10°$) during this event. THEMIS-B was in the solar wind just upstream from the bow shock (~17 R_E upstream of Earth, and ~10 R_E off the Sun-Earth line) during this interval and observed very similar IMF components. This suggests that the source of the TCV may again be an ion foreshock instability upstream of a quasi-parallel bow shock. The lack of significant perturbations in OMNI and THEMIS-B data (neither near the subsolar bow shock) is consistent with recent observations by *Zhang et al.* [2013] and *Engebretson et al.* [2013] and hybrid simulations by *Omidi et al.* [2013] that bow shock instabilities that are capable of causing transient pressure increases at the dayside magnetopause can occur even in the absence of significant solar wind perturbations.

3.3. Event 3: 4 October 2008

[24] Figure 4 shows a ~320 nT p-p amplitude TCV near 1410 UT on 4 October 2008 that was again accompanied by a Pc1 wave burst. Figures 4b, 4c, 4d, 4e, and 4f show search coil magnetometer data from Iqaluit and Sondrestromfjord in the northern hemisphere and from South Pole, AGO-P3, and AGO-P2 in the southern hemisphere. TCV signatures again

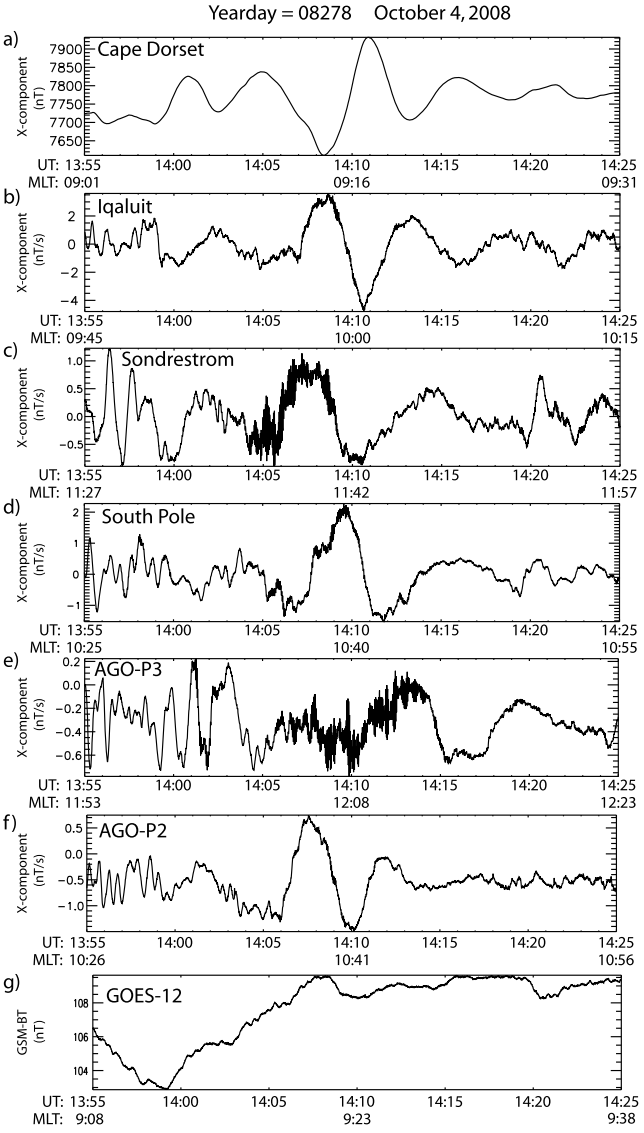

Figure 4. Line plots of X component data from 1355 to 1425 UT 4 October 2008 as in Figure 2. The dB/dt data from two northern hemisphere sites: (b) Iqaluit and (c) Sondrestromfjord and the dB/dt data from three Antarctic sites: (d) South Pole Station, (e) AGO-P3, and (f) AGO-P2.

Table 2. Amplitudes of the TCV and Pc1 Bursts Observed Near 1410 UT 4 October 2008[a]

Observing Station	MLAT (°)	MLT (HH:MM)	TCV Amplitude Fluxgate (nT)	Pc1 Amplitude Search Coil (nT/s)
South Pole	74.3	10:40	240	0.6
Sondrestromfjord	73.4	11:42	—	1.2
Cape Dorset	73.25	09:16	320	—
Iqaluit	72.1	10:00	100	1.3
AGO-P3	72.1	12:08	70	0.6
AGO-P2	70.2	10:41	85	<0.2

[a]Stations are listed in order of decreasing magnetic latitude (MLAT).

appeared in the search coil traces. In the northern hemisphere the long-period variations between 1405 and 1415 appeared 2–3 min earlier at Sondrestromfjord than at Iqaluit, consistent with westward and dawnward propagation at 3 km/s. The three southern hemisphere traces, each at a different magnetic latitude, did not show a clear temporal pattern. TCV signatures in the Cape Dorset and Iqaluit fluxgate data (not shown) also indicated westward (dawnward) TCV propagation with speeds of 2 km/s.

[25] During this TCV event, strong Pc1 waves occurred at all of these sites except AGO-P2 (located at the lowest latitude, 70° MLAT). Table 2 lists the amplitude of the TCV and Pc1 burst at each of these stations. The TCV amplitude distribution in latitude suggests a peak near 73° or 74° MLAT, with modestly decreasing amplitudes at lower latitudes. The Pc1 burst amplitude was largest at 72.1° and 73.4° MLAT, with amplitudes dropping off more quickly toward both higher and lower latitudes. However, a local time effect is also present in the Pc1 amplitude data. Figures 4c and 4d show that the ratio of Pc1 amplitude to TCV amplitude in search coil data was much larger at Sondrestromfjord and AGO-P3, the two stations nearest to local magnetic noon at the time of this event (1142 and 1208 MLT, respectively), than at the other stations. This pattern will also appear in the statistical results to be presented below. As in event 1, the Pc1 burst at these two stations occurred during the first half of the TCV, and an increase in the total magnetic field at GOES-12 near 1407 UT (Figure 4g) coincided with the TCV observed on the ground.

[26] Geomagnetic conditions during this event were again relatively quiet ($Kp = 2$ and $Dst = -16$ nT), but the available upstream data provide a complex picture. The OMNI solar wind velocity was ~ 590 km/s before and during this interval, but a 25% solar wind dynamic pressure increase (from 1.4 to 1.75 nPa) simultaneous with a rotation away from a mostly radial IMF occurred near 1405 UT. However, the IMF observed by THEMIS-B (located 16 R_E Sunward of Earth and ~25 R_E off the Sun-Earth line on the dawn flank) remained radial from 1300 to 1450 UT. THEMIS-C (located 15 R_E Sunward of Earth and within 7 R_E of the Sun-Earth line near 1000 local time) observed an outward moving bow shock excursion from ~1355 to 1410 UT, and THEMIS-D (located just inside the near-equatorial magnetopause at ~0930 local time) saw an inward excursion of the magnetopause past the spacecraft from 1406 to 1409 UT. The near-Earth THEMIS observations suggest the presence of an instability in the ion foreshock that was similar to events reported by *Korotova et al.* [2012] and *Engebretson et al.* [2013], but again the data are insufficient to determine what may have triggered the observed TCV and Pc1 burst.

3.4. Event 4: 7 August 2009

[27] A Pc1 burst was first identified in the Longyearbyen search coil data from 7 August 2009, and a nearly simultaneous TCV occurred at the same location and at the other IMAGE magnetometer sites on Svalbard (NAL and HOR). Figure 5a shows a clear ~80 nT p-p TCV in the east-west (Y component) magnetic field data from these stations at 0900 UT. An 8 nT/s p-p Pc1 burst was observed nearly simultaneously at LYR (Figure 5b). Figure 5c shows a 10 min expanded view of the Pc1 wave packet, indicating a series of ~30 to 50 s wave packets (in the Pc3-4 frequency band) within the ~5 min burst. Although the presence of Pc 3–4 pulsations during TCV events is not the focus of this study, we note that *Shields et al.* [2003] found that the joint occurrence rate of Pc 3–4 events and TCVs was between 70 and 90%.

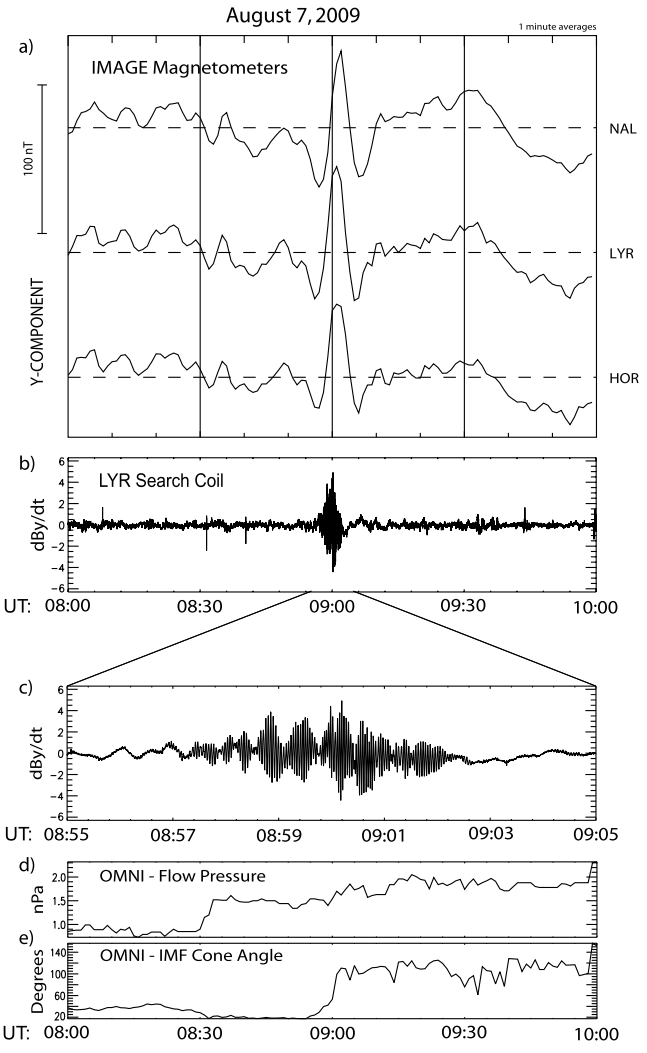

Figure 5. Line plots of magnetic field data and solar wind parameters from 0800 to 1000 UT 7 August 2009. (a) The Y component (east-west) of B from the three IMAGE magnetometer stations on Svalbard (NAL, LYR, and HOR, respectively). (b) The Y component (east-west) of dB/dt from the search coil at LYR, and (c) an expanded view of 10 min of this wave data. The time-shifted solar wind (d) flow pressure and (e) IMF cone angle, respectively, from the OMNI data base.

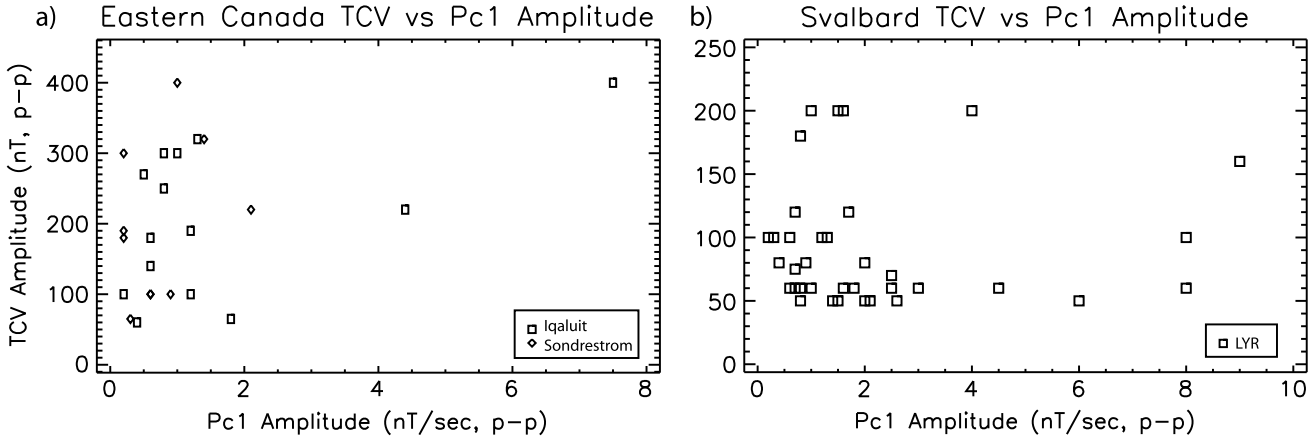

Figure 6. Plots of TCV amplitude versus the amplitude of Pc1 waves from two regions: (a) Eastern Canada and (b) Svalbard.

[28] Geomagnetic conditions during this event were again relatively quiet ($Kp = 1-$ and $Dst = -13$ nT) but upstream data again provided a complex picture. OMNI data for this event showed a ~0.5 nPa increase in solar wind pressure 30 min before the event, followed by a gradual increase throughout the event (Figure 5d). The IMF cone angle quickly increased at the time of the TCV and Pc1 burst, indicating a sharp field reorientation from quasi-parallel to quasi-perpendicular (Figure 5e). However, THEMIS-B, located ~29 R_E upstream of Earth, recorded the pressure increase at 0845 and the IMF reorientation at 0850 UT. Using the observed *Vsw* to time shift the THEMIS-B data by ~5 min, we estimate that the pressure increase reached the bow shock near 0850 and the IMF reorientation near 0855. The magnetopause moved inward past THEMIS-A and THEMIS-C, located in the outer afternoon magnetosphere near 1400 MLT, near 0852 UT, simultaneous with the beginning of a sharp 10 nT rise in the SYM-H index that peaked at 0902 UT. The nearer-Earth THEMIS observations thus suggest that either or both the pressure increase or the IMF cone angle change may have triggered this TCV/Pc1 burst event.

4. Statistical Analysis

[29] As noted in section 1, historically TCV events were identified first and Pc1 bursts were later identified in conjunction with them, and this sequence was followed in the earlier statistical studies of *Arnoldy et al*. [1988, 1996]. We followed this same identification sequence in analyzing the data from Eastern Canada, so that the occurrence results of these studies could be compared. In order to avoid the implicit bias in earlier studies of always identifying TCV events first and then searching for Pc1 bursts, however, we reversed this sequence in analyzing the Svalbard data.

[30] TCVs were identified first in magnetic perturbation data from Cape Dorset, and data from Iqaluit (~1 h MLT east of Cape Dorset, available for all but five of the events identified) or Repulse Bay (a MACCS station ~ 1 h MLT west of Cape Dorset, used for the remaining five events) were used to confirm that each candidate event exhibited longitudinal motion. Subsequently, search coil magnetometer data from Iqaluit, Sondrestromfjord, and South Pole were scanned for Pc1 bursts. (Data were not consistently available from AGO P2 and AGO P3, so their data were not included in the statistical study.) A total of 73 TCVs from Jan 2008 through July 2010 with amplitude ≥ 50 nT were identified in Cape Dorset data. Only 16 of these (22%) had simultaneous Pc1 bursts with amplitude ≥0.2 nT/s at one or more of the corresponding sites. This percentage is significantly lower than the 60% and 70% values obtained in the earlier studies of *Arnoldy et al*. [1988, 1996].

[31] The reverse procedure was followed at Svalbard: Pc1 events were identified first at LYR, and subsequently IMAGE array data were scanned for TCVs. In this case, 131 Pc1 bursts with amplitude ≥ 0.2 nT/s were identified. In 36 of these (27%), simultaneous TCVs with amplitude ≥ 50 nT were identified at the same location.

[32] The plots in Figure 6 show a comparison of amplitudes of TCVs and Pc1 bursts from both regions (Figure 6a: eastern Canada and Figure 6b: Svalbard). In neither case was there a clear correlation between amplitudes, much less a linear relationship. When TCVs were initially selected, most Pc1 bursts were of low amplitude (Figure 6a), and when Pc1 bursts were initially selected, TCVs were often observed but with highly variable amplitude (Figure 6b).

[33] Figure 7a shows the distribution of two categories of events in universal time observed in eastern Canada: (a) TCVs and (b) the subset of TCVs with Pc1 bursts. The red arrow indicates magnetic local noon for CD (used to identify TCVs) and the blue arrow indicates magnetic local noon for IQ (used to identify Pc1 bursts). The local time distribution of TCV events extended from 1000 to 2100 UT (5 to 16 MLT). The distribution of TCV events with Pc1 bursts, however, was more limited, extending only from 1300 to 1900 UT (±3 h from local noon). Both categories exhibited a deep minimum near local noon.

[34] Figure 7b, in a format similar to that of Figure 7a, shows the universal time distribution of Pc1 bursts (grey bars) and Pc1 bursts associated with TCVs (black bars) on Svalbard. The vertical black arrow indicates the UT of local magnetic noon at Longyearbyen (0856 UT). The local time extent of the distribution of Pc1 events is similar to that shown in Figure 7a, in that most events were observed within ±3 h of local noon (from 0600 to 1200 UT), although there is also a relatively small population extending from 1200 to 1800 UT. The distribution of Pc1 events with TCVs also has a minimum near local noon similar to that shown in Figure 7a.

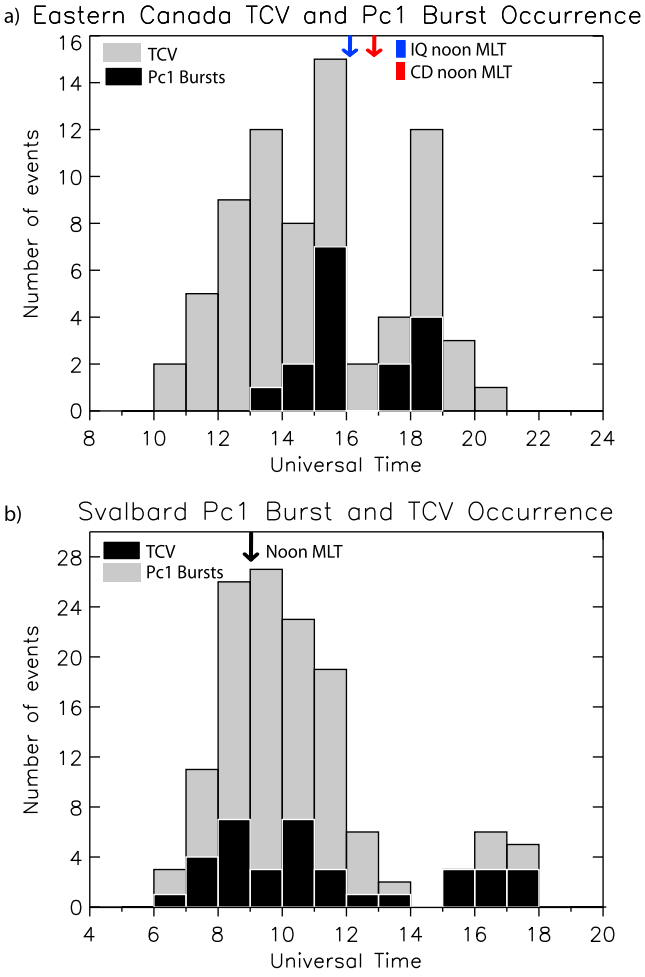

Figure 7. (a) Distribution of TCV events in universal time at Cape Dorset in eastern Canada. The top of the grey bars indicates the total number of events in each 1 h local time bin. Grey shading indicates TCV events without Pc1 bursts, and black shading indicates TCV events with a simultaneous Pc1 burst. The UT of local magnetic noon is indicated for Cape Dorset (red arrow) and Iqaluit (blue arrow). (b) Distribution of Pc1 burst events in universal time at Svalbard as in Figure 7a. Grey shading indicates Pc1 burst events without TCVs and black shading indicates Pc1 burst events with a simultaneous TCV. The UT of local magnetic noon is indicated by the vertical arrow.

[35] A significant feature of Figure 7b is the continuous distribution of Pc1 events across local noon; the distribution of Pc1 events without TCVs actually peaks within ± 1 h of local noon. This distribution is revealed because of the different identification sequence (Pc1 bursts first then TCVs) used for the Svalbard data.

[36] The foot point of the GOES-12 satellite was within 5 min MLT of Cape Dorset during the 2008–2010 time interval used in this study (Table 1). Simultaneous GOES-12 magnetic field data were available for 67 of the 74 TCV events in this study and were used to look for changes in the total magnetic field that could be associated with the TCVs identified in the Cape Dorset data. Of these 67 TCV events, 38 (57%) were associated with ≥2 nT increases in B at GOES-12, 28 (42%) showed increases from 0 to 2 nT, and one showed a decreasing total field.

[37] Figure 8 shows the local time distribution of the Cape Dorset TCV occurrences for which GOES-12 data were available (grey bars) and TCV with Pc1 bursts (black bars), as a function of MLT at GOES-12. Figure 8a is a histogram of TCV and TCV/Pc1 burst occurrence for events with a magnetic field increase of ≥2 nT at GOES-12. Figure 8b shows events with total field increases of < 2 nT at GOES-12. The one event for which the total field at GOES-12 decreased (at 13 MLT) is not included in either plot. The spread in local time of TCV events with and without simultaneous compressions at GOES-12 is quite similar, but the distribution of those with simultaneous compressions (Figure 8a) was more strongly peaked near (but not at) local magnetic noon. Both panels show occurrence minima within 1 h of local noon MLT, consistent with the parent TCV distribution shown in Figure 7a. Magnetic field compressions at GOES-12 are seen to occur during most of the TCV/Pc1 burst events (compare to Figure 7a); only two of the 14 TCV/Pc1 burst events for

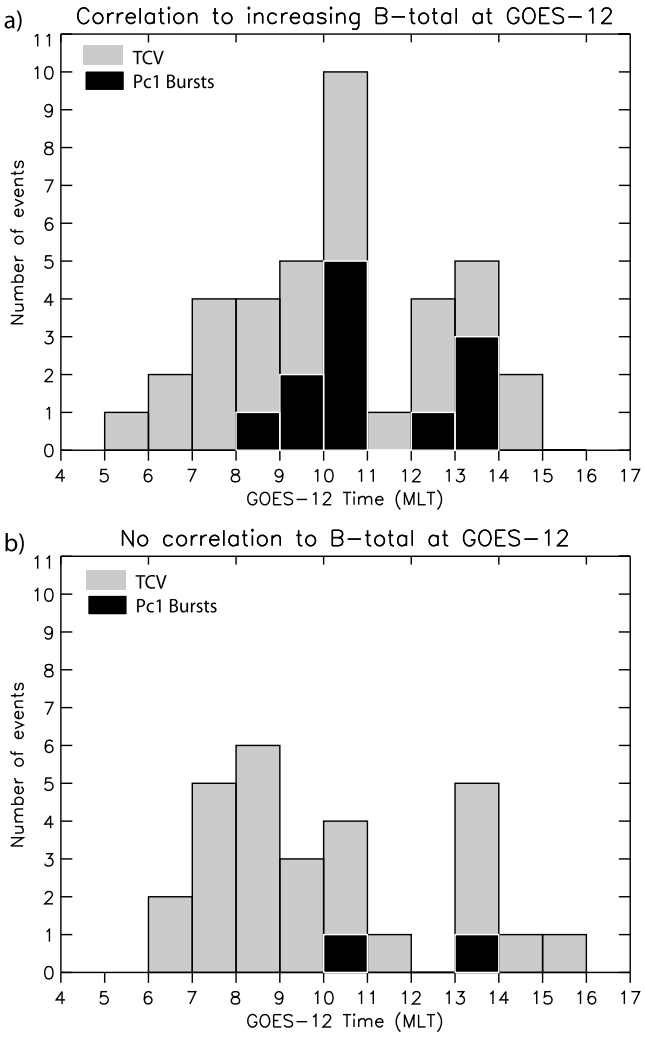

Figure 8. Local time distribution of events at Cape Dorset in eastern Canada as in Figure 7a. (a) Events simultaneous with increases in the total magnetic field ($\Delta B \geq 2$ nT) at GOES-12. (b) Events with no increase ($\Delta B < 2$ nT) in the total magnetic field at GOES-12.

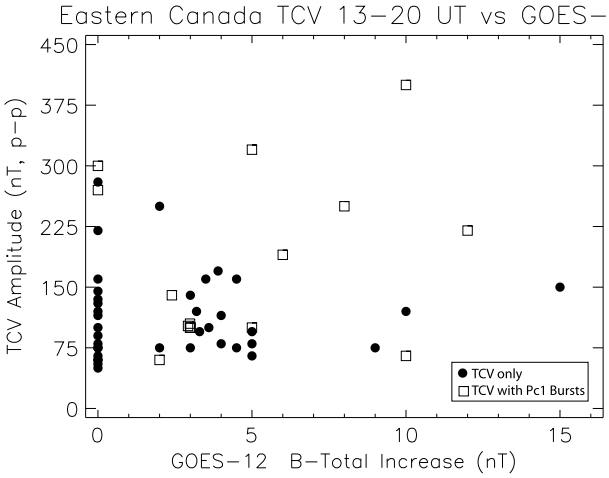

Figure 9. Distribution of TCV amplitudes at Cape Dorset for events observed between 1300 and 2000 UT, as a function of simultaneous increases in the total magnetic field at GOES-12. The solid circles represent TCV-only events, and open squares represent TCVs simultaneous with Pc1 bursts.

which GOES-12 data were available were not accompanied by ≥ 2 nT compressions.

[38] A comparison of TCV amplitude to increases in total field data from the GOES-12 satellite magnetometer is shown in Figure 9. There is little evident correlation between TCV amplitude and the magnitude of the magnetic field compression at GOES-12. The TCVs with Pc1 bursts (open squares) do show a modest tendency to occur with the stronger TCVs and field compressions but not in all cases.

5. Discussion

[39] In two previous studies [*Arnoldy et al*., 1988, 1996], Pc1 burst events (wave packets with frequencies near 0.5 Hz) were identified during 50 to 70% of traveling convection vortex (TCV) events (solitary waves with frequencies near 2–5 mHz) observed at high latitude ground stations during daytime hours. By looking for the presence of TCVs and Pc1 bursts in two different sequences (identifying TCVs first in Eastern Canada and then looking for simultaneous Pc1 bursts, and identifying Pc1 bursts first in Svalbard and then looking for simultaneous TCVs), we have found a considerably weaker association between TCVs and Pc1 bursts, with a relatively low percentage of events occurring simultaneously. When TCV events were identified first, Pc1 bursts appeared simultaneously with 22% of the TCVs. When Pc1 bursts were identified first, TCVs appeared simultaneously with 27% of the Pc1 bursts.

[40] Comparisons of the occurrences of TCV/Pc1 bursts and magnetic field compressions at geosynchronous orbit at the same magnetic local time also revealed a complex pattern. Not surprisingly, relatively more TCV events without GOES-12 field compressions occurred at local times farther from local noon; at these local times the signature of the transient compression in the GOES-12 data was more likely to be a twist of the magnetic field (consistent with a localized, transient field-aligned current). Perhaps more significantly, field compressions at GOES-12 were more likely to occur when Pc1 bursts accompanied TCVs. This is consistent with our current understanding that compressions of the magnetic field, but not twists (and their associated field-aligned currents), are effective in increasing the instability of outer dayside magnetospheric ion populations to electromagnetic ion cyclotron waves [*Olson and Lee*, 1983; *Kangas et al*., 1998].

[41] We have also noted the similarity in local time distributions for TCVs associated with Pc1s in the two data sets presented here. By selecting TCV events first and then looking for simultaneous Pc1 wave bursts, we found a sharp minimum in event occurrence very near local noon. In contrast, by selecting Pc1 burst events first and then looking for simultaneous TCV events, we found a distribution of Pc1 bursts that peaked near local noon, but a distribution of Pc1 bursts simultaneous with TCVs that again showed a near-noon minimum. The relative absence of TCV events very close to local noon is consistent with some earlier studies of these events [e.g., *Lanzerotti et al*., 1991 and *Sibeck and Korotova*, 1996], and is typified by event 3 (Figure 4 and Table 2): the TCV amplitudes were weaker relative to Pc1 burst amplitudes at stations very near to local noon. Many statistical studies, however, did not report a minimum near local noon, including the *Zesta et al*. [2002] study, which also used MACCS data, and *Moretto et al*. [2004], who used data from both the eastern and western coasts of Greenland. As *Zesta et al*. [2002] pointed out, the selection criteria influence both the occurrence rate and the diurnal distribution. The selection criteria used for the MACCS events in this study followed those of *Zesta et al*. [2002] in all but one important way: Whereas that study required a TCV signature in at least two of the three available longitudinally separated stations (Pangnirtung, Cape Dorset, and Repulse Bay), in this study events were identified at only one station (Cape Dorset), and were confirmed to be TCVs when observed at another station located ±1 h in MLT. As *Zesta et al*. [2002] noted, both the event study of *Zesta et al*. [1999] and the simulation work of *Lysak et al*. [1994] indicated that TCVs were weaker when created in the local noon region and strengthened as they moved longitudinally away from their point of creation. *Lühr and Blawert* [1994] reached a similar conclusion that the strongest TCV events were generally observed 2 to 3 h away from local noon.

[42] The statistical study of *Moretto et al*. [2004], which also required a TCV signature in two longitudinally separated regions, illustrated the complexity of the spatial pattern of these events. Their statistical results, like those of *Zesta et al*. [2002], showed no near-noon minimum in TCV occurrence but also revealed a magnetic latitude effect: observations from latitudes below ~75° yield a peak in local morning and a secondary peak in early afternoon, while observations from higher latitudes resulted in a single broad peak in late morning. Both this latitudinal effect and the conclusion cited above, that newly created TCVs in the local noon region are weaker, may contribute to the sharp minimum in TCV events observed at Cape Dorset (73.25° MLAT) near local noon.

[43] We have also confirmed that there is no linear relationship between the amplitudes of these two wave phenomena regardless of event selection of identifying TCVs first or Pc1 waves first. This is also consistent with our current understanding of EMIC wave generation: only under certain conditions is the plasma in the outer dayside magnetosphere sufficiently unstable that field compressions will generate these waves [*Anderson and Hamilton*, 1993].

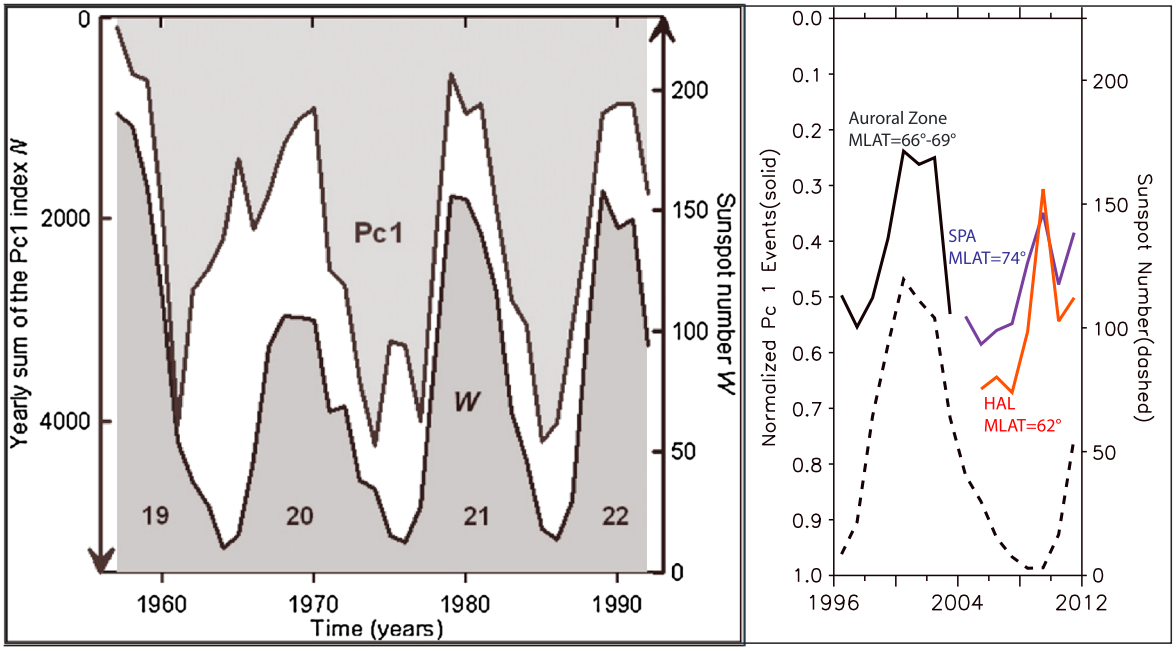

Figure 10. Composite figure showing the anticorrelation between annual rates of Pc1 wave occurrence and sunspot activity over several solar cycles. In Figure 10 (left) [*Guglielmi et al.*, 2006], which covers nearly four solar cycles, the yearly sum of Pc1 activity increases from the top down according to the scale on the left and the sunspot number increases from the bottom according to the scale on the right. The more recent data shown in Figure 10 (right) is described in the text.

[44] Finally, we note that the percentage of TCVs accompanied by Pc1 bursts during the interval of this study (2008 to mid-2010) was considerably lower than the percentages found by *Arnoldy et al.* [1988, 1996], who visually identified isolated TCVs of amplitude ≥100 nT (a stricter criterion than used in this study) and simultaneous Pc1 bursts. Although the Cape Dorset station in Eastern Canada used to identify TCVs in this study is located ~1 h MLT west of the Iqaluit/South Pole station pair used by *Arnoldy et al.* [1988, 1996], the TCVs were in nearly all cases also identified at Iqaluit. The TCV observed at Cape Dorset was also observed at Iqaluit in each of the 68 cases (of 73) for which Iqaluit data were available. For the other five cases, the TCVs at Cape Dorset were also seen at Repulse Bay, located to the west of Cape Dorset. This suggests that the difference in station used to identify TCVs was probably not the primary factor causing the difference in occurrence percentages. We instead attribute this lower percentage to the overall anomalously low occurrence of Pc1 waves at both middle and high latitudes during the most recent solar minimum period. As will be shown in Figure 10, during each of the five previous solar cycles, Pc1 wave occurrence was anticorrelated with sunspot number. That is, ground-based Pc1 wave occurrences more than doubled between years of solar maximum and solar minimum. From 2008 to 2010, however, both sunspot and Pc1 wave activity were very low.

[45] A negative correlation between the occurrence of ULF waves in the Pc1 frequency range and sunspot numbers was first reported by *Benioff* [1960], based on 4 years of data from southern California. Since then, a number of studies at low, middle, and high magnetic latitudes (reviewed by *Mursula et al.* [1991]), many with longer baselines, have reported similar anticorrelations. The two studies with the longest baselines, *Mursula et al.* [1991] and *Guglielmi et al.* [2006], both covered more than three solar cycles.

[46] *Mursula et al.* [1991] found a very strong negative correlation between annual Pc1 activity and the annual sunspot number at Sodankylä, Finland ($L = 5.2$) over nearly four solar cycles (from 1932 to 1944 and 1959 to 1983).

[47] Figure 10 (left) shows the strong anticorrelation between the sunspot number, shown on the right-hand scale, with 0 at the bottom, and the yearly Pc1 index from Borok, Russia ($L = 2.9$), shown on the left-hand scale, with 0 at the top, based on continuous data from 1957 to 1992. The two variables exhibit a clear anticorrelation, with correlation coefficient $r = -0.83$ [*Guglielmi et al.*, 2006].

[48] Figure 10 (right), also with inverted scales for Pc1 activity, incorporates observations from the Augsburg College/University of New Hampshire search coil magnetometers at three automated observatories at auroral zone latitudes operated by the British Antarctic Survey (BAS) for 8 years (1996 through 2003) [*Posch et al.*, 2010] and similar instruments at South Pole Station (2004–2011) and Halley (2005–2011), Antarctica. The BAS AGO auroral zone observations clearly continue the pattern shown in Figure 10 (left), but the Halley data deviate sharply from this pattern beginning in 2008, as do the higher-latitude South Pole data.

[49] *Guglielmi et al.* [2006] noted that the commonly accepted mechanism for the earlier solar cycle variation was the 11 year variation of O^+ ions in the magnetosphere, which increases as a result of increasing solar activity [*Young et al.*, 1982]. No corresponding increase of O^+ ions would be expected in the magnetosphere during the deep solar minimum of 2008–2010, however. We instead speculate that the deep minimum in magnetospheric convection during this period

led to a significant reduction in dayside ring current and plasma sheet ion populations. This would in turn reduce the likelihood that TCV-related compressions would stimulate EMIC waves.

[50] In future work we intend to follow up on the current study by independently identifying TCV and Pc1 bursts at both the Eastern Canada and Svalbard sites during the more active solar and geomagnetic conditions from 2011 through 2013, in order to both further clarify the statistical associations reported here and determine whether the long-term anticorrelation of Pc1 wave occurrence with solar activity reappears in this newer data set.

[51] **Acknowledgments.** This research was supported by NSF grants ATM-0827903, ANT-0838917, ANT-0840133, and ARC-0806196 to Augsburg College, and grants ANT-0839938, ANT-0838910, and ARC-0806338 to the University of New Hampshire. Work by M.D.H. was supported by NSF grant AGS-1230398. The identification of events at Svalbard was performed while M.J.E. was a visitor at the University of Oslo, supported by a grant from the Norwegian Research Council. The Magnetometer Array for Cusp and Cleft Studies (MACCS), Arctic Canada, is operated by Augsburg College. Search coil magnetometers at Iqaluit, Sondrestromfjord, South Pole, Antarctic AGOs, and four sites in Svalbard are operated jointly by Augsburg College and the University of New Hampshire. We thank the institutes who maintain the IMAGE Magnetometer Array. HOR is owned and operated by the Institute of Geophysics of the Polish Academy of Science and NAL and LYR by the Tromsø Geophysical Observatory at the University of Tromsø, Norway. GOES satellite data are supplied by the Space Weather Prediction Center, NOAA, Boulder, CO. The OMNI data are supplied by OMNIWeb Plus, Space Physics Data Facility, NASA/Goddard Space Flight Center, Greenbelt, MD. We thank Harald Frey for helpful discussions.

[52] Robert Lysak thanks Therese Moretto and Robert Clauer for their assistance in evaluating this paper.

References

Anderson, B. J., and D. C. Hamilton (1993), Electromagnetic ion cyclotron waves stimulated by modest magnetospheric compressions, *J. Geophys. Res.*, *98*, 11,369–11,382, doi:10.1029/93JA00605.

Arnoldy, R. L., M. J. Engebretson, and L. J. Cahill Jr. (1988), Bursts of Pc 1–2 near the ionospheric footprint of the cusp and their relationship to flux transfer events, *J. Geophys. Res.*, *93*, 1007–1016.

Arnoldy, R. L., M. J. Engebretson, J. L. Alford, R. E. Erlandson, and B. J. Anderson (1996), Magnetic impulse events and associated Pc 1 bursts at dayside high latitudes, *J. Geophys. Res.*, *101*(A4), 7793–7799, doi:10.1029/95JA03378.

Benioff, H. (1960), Observations of geomagnetic fluctuations in the period range 0.3 to 120 seconds, *J. Geophys. Res.*, *65*, 1413–1422.

Engebretson, M. J., W. J. Hughes, J. L. Alford, E. Zesta, L. J. Cahill Jr., R. L. Arnoldy, and G. D. Reeves (1995), Magnetometer array for cusp and cleft studies observations of the spatial extent of broadband ULF magnetic pulsations at cusp/cleft latitudes, *J. Geophys. Res.*, *100*(A10), 19,371–19,386, doi:10.1029/95JA00768.

Engebretson, M. J., et al. (1997), The United States automatic geophysical observatory (AGO) program in Antarctica, in *Satellite—Ground Based Coordination Sourcebook, ESA-SP-1198*, edited by M. Lockwood, M. N. Wild, and H. J. Opgenoorth, pp. 65–99, ESA Publications, ESTEC, Noordwijk, The Netherlands.

Engebretson, M. J., J. Moen, J. L. Posch, F. Lu, M. R. Lessard, H. Kim, and D. A. Lorentzen (2009), Searching for ULF signatures of the cusp: Observations from search coil magnetometers and auroral imagers in Svalbard, *J. Geophys. Res.*, *114*, A06217, doi:10.1029/2009JA014278.

Engebretson, M. J., et al. (2013), Multi-instrument observations from Svalbard of a traveling convection vortex, electromagnetic ion cyclotron wave burst, and proton precipitation associated with a bow shock instability, *J. Geophys. Res. Space Physics*, *118*, doi:10.1002/jgra.50291.

Fairfield, D. H., W. Baumjohann, G. Paschmann, H. Lühr, and D. G. Sibeck (1990), Upstream pressure variations associated with the bow shock and their effects on the magnetosphere, *J. Geophys. Res.*, *95*, 3773–3786, doi:10.1029/JA095iA04p03773.

Fillingim, M. O., J. P. Eastwood, G. K. Parks, V. Angelopoulos, I. R. Mann, S. B. Mende, and A. T. Weatherwax (2011), Polar UVI and THEMIS GMAG observations of the ionospheric response to a hot flow anomaly, *J. Atmos. Sol.-Terr. Phys.*, *73*, 137–145.

Friis-Christensen, E., M. A. McHenry, C. R. Clauer, and S. Vennerstrøm (1988), Ionospheric traveling convection vortices observed near the polar cleft: A triggered response to sudden changes in the solar wind, *Geophys. Res. Lett.*, *15*, 253–256, doi:10.1029/GL015i003p00253.

Glassmeier, K.-H., M. Hönisch, and J. Untiedt (1989), Ground-based and satellite observations of traveling magnetospheric convection twin vortices, *J. Geophys. Res.*, *94*, 2520–2528.

Guglielmi, A., A. Potapov, E. Matveyeva, T. Polyushkina, and J. Kangas (2006), Temporal and spatial characteristics of Pc1 geomagnetic pulsations, *Adv. Space Res.*, *38*, 1572–1575.

Hughes, W. J., M. J. Engebretson, and E. Zesta (1995), Ground observations of transient cusp phenomena: Initial results from MACCS, in *Physics of the Magnetopause; Geophysical Monograph 90*, edited by P. Song, B. U. O. Sonnerup, and M. F. Thomsen, pp. 427–437, American Geophysical Union, Washington, D.C.

Kangas, J., A. Guglielmi, and O. Pokhotelov (1998), Morphology and physics of short-period geomagnetic pulsations, *Space. Sci. Rev.*, *83*, 435–512, doi:10.1023/A:1005063911643.

Kataoka, R., H. Fukunishi, and L. J. Lanzerotti (2003), Statistical identification of solar wind origins of magnetic impulse events, *J. Geophys. Res.*, *108*(A12), 1436, doi:10.1029/2003JA010202.

Kivelson, M. G., and D. J. Southwood (1991), Ionospheric traveling vortex generation by solar wind buffeting of the magnetosphere, *J. Geophys. Res.*, *96*, 1661–1667, doi:10.1029/90JA01805.

Korotova, G. I., D. G. Sibeck, N. Omidi, and V. Angelopoulos (2012), THEMIS observations of unusual bow shock motion attending a transient magnetospheric event, *J. Geophys. Res.*, *117*, A12207, doi:10.1029/2012JA017510.

Lanzerotti, L. J., R. M. Konik, A. Wolfe, D. Venkatesan, and C. G. Maclennan (1991), Cusp latitude magnetic impulse events: 1. Occurrence statistics, *J. Geophys. Res.*, *96*, 14,009–14,022, doi:10.1029/91JA00567.

Lühr, H. (1994), The IMAGE magnetometer network, *STEP Int.*, *4*(10), 4–6.

Lühr, H., and W. Blawert (1994), Ground signatures of travelling convection vortices, in *Solar Wind Sources of Magnetospheric Ultra-Low-Frequency Waves*, Geophys. Monogr. Ser., vol. 81, edited by M. J. Engebretson, K. Takahashi, and M. Scholer, pp. 231–251, AGU, Washington, D.C.

Lühr, H., M. Lockwood, P. E. Sandholt, T. L. Hansen, and T. Moretto (1996), Multi-instrument ground-based observations of a travelling convection vortices event, *Ann. Geophys.*, *14*, 162–181, doi:10.1007/s00585-996-0162-z.

Lysak, R. L., Y. Song, and D.-H. Lee (1994), Generation of ULF waves by fluctuations in the magnetopause position, in *Solar Wind Sources of Magnetospheric ULF Waves*, Geophys. Monogr. Ser., vol. 81, edited by M. J. Engebretson, K. Takahashi, and M. Scholer, pp. 273–281, AGU, Washington, D.C.

Massetti, S. (2005), Dayside magnetosphere-ionosphere coupling during IMF clock angle ~90°: Longitudinal cusp bifurcation, quasi-periodic cusp-like auroras, and traveling convection vortices, *J. Geophys. Res.*, *110*, A07304, doi:10.1029/2004JA010965.

McHenry, M. A., and C. R. Clauer (1987), Modeled ground magnetic signatures of flux transfer events, *J. Geophys. Res.*, *92*, 11,231–11,240, doi:10.1029/JA092iA10p11231.

Mende, S. B., R. L. Rairden, L. J. Lanzerotti, and C. G. Maclennan (1990), Magnetic impulses and associated optical signatures in the dayside aurora, *Geophys. Res. Lett.*, *17*, 131–134, doi:10.1029/GL017i002p00131.

Mende, S. B., H. U. Frey, J. H. Doolittle, L. Lanzerotti, and C. G. Maclennan (2001), Dayside optical and magnetic correlation events, *J. Geophys. Res.*, *106*, 24,637–24,649, doi:10.1029/2001JA900065.

Moretto, T., M. Hesse, A. Yahnin, A. Ieda, D. Murr, and J. F. Watermann (2002), Magnetospheric signature of an ionospheric travelling convection vortex event, *J. Geophys. Res.*, *107*(A6), 1072, doi:10.1029/2001JA000049.

Moretto, T., D. G. Sibeck, and J. F. Watermann (2004), Occurrence statistics of magnetic impulsive events, *Ann. Geophys.*, *22*, 585–602, doi:10.5194/angeo-22-585-2004.

Murr, D. L., W. J. Hughes, A. S. Rodger, E. Zesta, H. U. Frey, and A. T. Weatherwax (2002), Conjugate observations of traveling convection vortices: The field-aligned current system, *J. Geophys. Res.*, *107*(A10), 1306, doi:10.1029/2002JA009456.

Murr, D. L., and W. J. Hughes (2003), Solar wind drivers of traveling convection vortices, *Geophys. Res. Lett.*, *30*(7), 1354, doi:10.1029/2002GL015498.

Mursula, K., J. Kangas, and T. Pikkarainen (1991), Pc1 micropulsations at a high-latitude station: A study over nearly four solar cycles, *J. Geophys. Res.*, *96*, 17,651–17,661.

Olson, J. V., and L. C. Lee (1983), Pc 1 wave generation by sudden impulses, *Planet. Space Sci.*, *31*, 295–302.

Omidi, N., H. Zhang, D. Sibeck, and D. Turner (2013), Spontaneous hot flow anomalies at quasi-parallel shocks, 2, Hybrid simulations, *J. Geophys. Res. Space Physics*, *118*, 173–180, doi:10.1029/2012JA018099.

Pilipenko, V. A., S. L. Shalimov, E. N. Fedorov, M. J. Engebretson, and W. J. Hughes (1999), Coupling between field-aligned current impulses and Pi 1 noise bursts, *J. Geophys. Res.*, *104*, 17,419–17,430.

Posch, J. L., M. J. Engebretson, M. T. Murphy, M. H. Denton, M. R. Lessard, and R. B. Horne (2010), Probing the relationship between EMIC waves and plasmaspheric plumes near geosynchronous orbit, *J. Geophys. Res. 115*, A11205, doi:10.1029/2010JA015446.

Russell, C. T., and R. C. Elphic (1979), ISEE observations of flux transfer events at the dayside magnetopause, *Geophys. Res. Lett.*, *6*, 33–36, doi:10.1029/GL006i001p00033.

Sanny, J., D. Berube, and D. G. Sibeck (2001), A statistical study of transient event motion at geosynchronous orbit, *J. Geophys. Res.*, *106*, 21,217–21,229, doi:10.1029/2000JA000394.

Shields, D. W., et al. (2003), Multistation studies of the simultaneous occurrence rate of Pc 3 micropulsations and magnetic impulsive events, *J. Geophys. Res.*, *108*(A6), 1225, doi:10.1029/2002JA009397.

Sibeck, D. G., and G. I. Korotova (1996), Occurrence patterns for transient magnetic field signatures at high latitudes, *J. Geophys. Res.*, *101*, 1313–1328, doi:10.1029/96JA00187.

Singer, H. J., L. Matheson, R. Grubb, A. Newman, and S. D. Bouwer (1996), Monitoring space weather with the GOES magnetometers, in *SPIE Conference Proceedings, GOES-8 and Beyond*, vol. 2812, edited by E. R. Washwell, pp. 299–308. [Available online at http://proceedings.spiedigitallibrary.org/volume.aspx?volume=2812.]

Sitar, R. J., J. B. Baker, C. R. Clauer, A. J. Ridley, J. A. Cumnock, V. O. Papitashvili, J. Spann, M. J. Brittnacher, and G. K. Parks (1998), Multi-instrument analysis of the ionospheric signatures of a hot flow anomaly occurring on July 24, 1996, *J. Geophys. Res.*, *103*(A10), 23,357–23,372, doi:10.1029/98JA01916.

Vorobjev, V. G., O. I. Yagodkina, and V. L. Zverev (1999), Morphological features of bipolar magnetic impulsive events and associated interplanetary medium signatures, *J. Geophys. Res.*, *104*, 4595–4607.

Vorobjev, V. G., O. I. Yagodkina, D. G. Sibeck, K. Liou, and C.-I. Meng (2001), Polar UVI observations of dayside auroral transient events, *J. Geophys. Res.*, *106*, 28,897–28,911, doi:10.1029/2000JA000396.

Young, D. T., H. Balsiger, and J. Geiss (1982), Correlations of magnetospheric ion composition with geomagnetic and solar activity, *J. Geophys. Res.*, *87*, 9077–9096, doi:10.1029/JA087iA11p09077.

Zesta, E., W. J. Hughes, M. J. Engebretson, T. J. Hughes, A. J. Lazarus, and K. I. Paularena (1999), The November 9, 1993 traveling convection vortex event: A case study, *J. Geophys. Res.*, *104*, 28,041–28,058.

Zesta, E., W. J. Hughes, and M. J. Engebretson (2002), A statistical study of traveling convection vortices using the Magnetometer Array for Cusp and Cleft Studies, *J. Geophys. Res.*, *107*(A10), 1317, doi:10.1029/1999JA000386.

Zhang, H., D. G. Sibeck, Q.-G. Zong, N. Omidi, D. Turner, and L. B. N. Clausen (2013), Spontaneous hot flow anomalies at quasi-parallel shocks, 1, Observations, *J. Geophys. Res. Space Physics*, *118*, 3357–3363, doi:10.1002/jgra.50376.